Strain in a single ultrathin silicon layer on top of SiGe islands: Raman spectroscopy and simulations

E. Bonera,[1] F. Pezzoli,[2] A. Picco,[1] G. Vastola,[1] M. Stoffel,[2] E. Grilli,[1] M. Guzzi,[1]
A. Rastelli,[2] O. G. Schmidt,[2] and L. Miglio[1]
[1]*Dipartimento di Scienza dei Materiali, and L-NESS, Università degli Studi di Milano-Bicocca, via Cozzi 53, I-20125 Milano, Italy*
[2]*IFW-Dresden, Institute for Integrative Nanosciences, Helmholtzstrasse 20, D-01069 Dresden, Germany*
(Received 10 November 2008; published 25 February 2009)

By means of resonant Raman spectroscopy we investigated the strain on a single ultrathin crystalline silicon layer, locally induced by buried SiGe nanostructures. The spectrum of a 5-nm-thick silicon layer on top of SiGe islands shows a single highly strained feature attributed to the out-of-plane phonon. The direct comparison of the experimental results with finite-element methods through spectral simulation shows excellent agreement that clarifies the physical origin of the spectrum. An increase in the silicon layer thickness up to 40 nm results in a progressive reduction in the strain.

DOI: 10.1103/PhysRevB.79.075321 PACS number(s): 81.07.−b, 61.46.−w, 71.15.Pd, 78.30.−j

I. INTRODUCTION

The investigation of the strain field in a semiconductor layer deformed by underlying nanostructures presents challenging issues from both the fundamental and application-related points of view. The experimental characterization is difficult because of the small dimensions, and the interpretation of the data is complicated due to the geometry of the system. Although the strain induced by a lattice mismatch between planar films is well known and also the problem of the strain induced in a planar layer by a pointlike source can be solved analytically, it is nevertheless hard to set an extent up to where these approximations can be used. A particularly relevant case is the experimental determination and interpretation of the Raman spectrum of an ultrathin silicon layer, locally strained by buried SiGe islands. These systems gained practical interest because strained silicon can provide increased charge-carrier mobility[1] and is fully compatible with mainstream Si technology.[2] Very recently, promising results have been obtained using buried $Si_{1-x}Ge_x$ nanostructures as local stressors to enhance Si-based device performance.[3] The possibility of achieving laterally ordered $Si_{1-x}Ge_x$ islands[4] is therefore a promising approach to realize dot-based field-effect transistors on Si.[5] The advantage over flat SiGe layers grown on Si is that 3D islands can be grown without dislocations with a substantially larger Ge concentration, and the different geometry allows the introduction of a much higher strain.

In such systems, one fundamental issue is therefore to control the strain within the Si layer. This aim requires the development of accurate and sensitive analytical methods. For the case of strain in ultrathin Si layers (around 10 nm), resonant Raman spectroscopy is particularly well suited for its sensitivity, nondestructivity, submicron lateral spatial resolution, and few-nanometer depth resolution. In this paper, we focus on the strain induced locally in a 5 nm Si layer on top of a buried SiGe island. For this system, although powerful, Raman spectroscopy is only qualitative in the absence of a model for interpretation because a nontrivial relationship links the strain tensor and the observable phonon energy shifts.[6] Therefore emphasis is given to the quantitative modeling of the experimental results in terms of the unfolding of the physical origin of the Raman spectra. This objective is pursued by the direct comparison of the experimental results with spectral simulation based on dedicated three-dimensional finite-element models (FEMs). Finally, the results from similar thicker layers of 10, 20, and 40 nm complete the picture showing an increasing relaxation of the films toward bulk values.

II. EXPERIMENTAL AND COMPUTATIONAL DETAILS

The samples presented in this work were grown by solid source molecular-beam epitaxy on *p*-Si(001) substrates. After standard deoxidation and buffer growth, 6.7 monolayers of Ge were deposited at 620 °C, leading to island nucleation. At this point, for the reference sample (0 nm cap) the substrate temperature was ramped to room temperature, while for the other samples the temperature was set to 300 °C before initiating the Si capping. Within these conditions, the overgrowth is conformal and the intermixing between the Si overlayers and the SiGe islands is almost completely suppressed.[7] We investigated the island shape, density, and distribution by atomic force microscopy (AFM) operating in tapping mode. Micro-Raman spectroscopy was performed on a Jasco R800 double spectrometer connected to an ultraviolet microscope. The spectral pitch of the array detector was 0.3 cm^{-1}. The geometry employed was backscattering from (001), with polarized excitation along (110) and unpolarized collection. The 363.8 nm excitation was focused by a 0.5 numerical aperture (NA) objective on a spot of 1 μm^2, illuminating about ten islands. The power was kept below 1 mW (corresponding to a density of 10^9 W m^{-2}) to prevent heating. Finite-element simulations were carried out with the COMSOL MULTIPHYSICS package. A realistic dome-shaped island was placed on a Si(001) substrate with four different Si capping layers on top of it. The concentration of the $Si_{1-x}Ge_x$ island was set to $x=0.60$ in accordance with the average experimental concentration.[8,9] Previous work showed that the relaxation at the surface is similar for an island with an

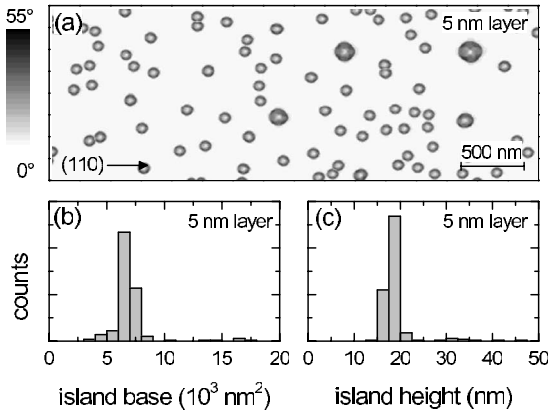

FIG. 1. (a) Atomic force microscopy scan of SiGe islands overgrown with a 5-nm-thick Si layer. The shading is proportional to the local surface slope with respect to the (001) plane. The buried nanostructures are uniform dome-shaped islands, coexisting with a negligible number of barn and superdome-shaped islands. A statistical analysis of island base area and height is shown in (b) and (c), respectively.

inhomogeneous Ge distribution and a uniform island with the same average concentration.[10] Lateral boundary conditions were applied to the simulation cell, while the bottom surface was kept fixed to mimic the semi-infinite bulk. Geometric multigrid algorithm was applied to solve the elastic problem and obtain the full strain tensor.

III. RESULTS AND DISCUSSION

The morphological analysis of the sample is based on statistical analysis of AFM images. Figure 1(a) shows for the 5 nm capped samples nearly uniform dome-shaped islands. The statistical distributions of the islands shown in panels (b) and (c) indicate that the dome base diameter is slightly less than 100 nm and the height is between 15 and 20 nm. Similar results were obtained for the other samples.

The analysis of the strain in the Si layer locally induced by the nanostructures is based on the Raman spectra shown in Fig. 2. Excitation at 3.4 eV is particularly suited for the investigation of strain in ultrathin Si films for two reasons. First, the resonance effect enhances the Raman scattering probability up to 30 times with respect to other accessible excitations,[11] which yields a signal-to-noise ratio high enough to perform spectral subtraction, i.e., the subtraction of a reference spectrum from the sample spectrum. Second, the limited penetration depth $d_p = 10$ nm limits the averaging to the upper $d_p/2$ thick skin, a dimension comparable to the thickness of our layers. The investigated area is about 1 μm^2, averaging among several islands simultaneously.

The spectrum of the bare SiGe nanostructures, indicated by 0 nm, shows a nearly flat response. A first result emerging from this measurement is the confirmation that the islands themselves are not detectable since none of the three SiGe bands is observed. Since the Si away from the islands is almost completely relaxed, this subtraction spectrum should be zero everywhere. The oscillations observed around the zero-shift energy are therefore indistinguishable from an artifact generated by the subtraction process. This artifact is most likely caused by an instrumental drift too small to be corrected by reference lines and corrupts the spectrum in a spectral region centered at 520.5 cm^{-1}, about 5 cm^{-1} wide. In the following discussion, we will ignore this part of the spectrum.

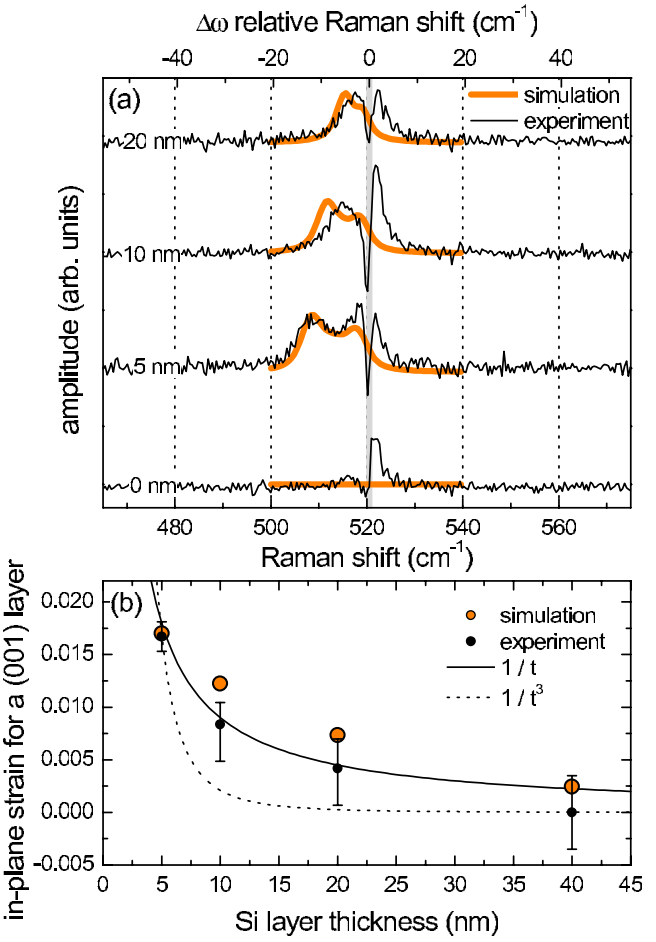

FIG. 2. (Color online) (a) Subtractive Raman spectra of a single ultrathin layer of silicon on top of SiGe nanostructures. The vertical solid line marks the unstrained value of 520.5 cm^{-1}. The region close to this value is corrupted by an artifact of the subtraction process. (b) Corresponding in-plane strain obtained by assuming that there is the same linear relationship between $\Delta\omega$ and ϵ as in the case of a flat (001) surface. The validity of this assumption is discussed in the text. The two solid lines show the $1/t$ behavior from Ref. 18 and the $1/t^3$ predicted by an analytical model (Ref. 19).

The 5 nm sample shows a band positioned at 508 cm^{-1}, well separated from the artifact region, superimposed to a shoulder, with a full width at half maximum (FWHM) of 6 cm^{-1}. If we assume that the Raman spectrum originates from a thin layer pseudomorphic to a flat (001) surface, this shift $\Delta\omega$ could be linearly related to a value of ϵ_{xx} component of 0.017,[12] as reported in Fig. 2(b). Unfortunately, this assumption can be valid only for the apex (001)-like surface of the dome, which contributes only for a small area with respect to the whole island. In a more realistic picture there are facets also along the (1 0 5), (1 1 3), and (15 3 23) planes, each of them contributing with its own Raman spectrum and selection rules, and the strain can in principle show complex

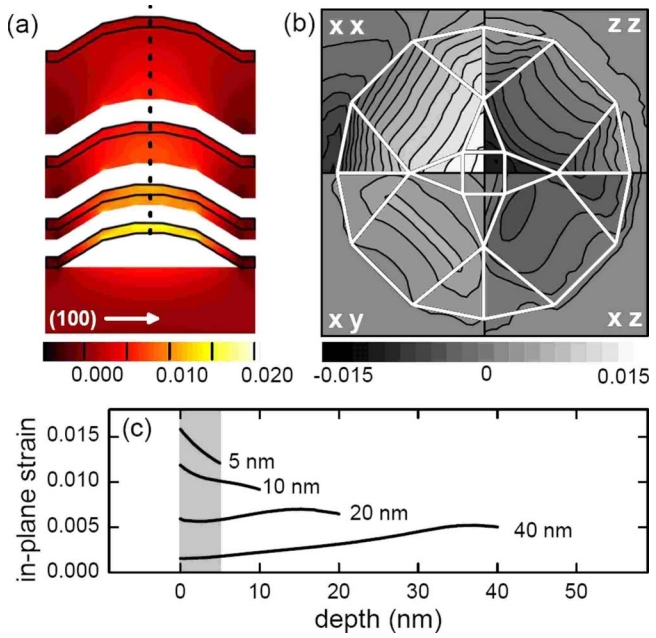

FIG. 3. (Color online) (a) Cross-sectional images of the map of the $(\epsilon_{xx}+\epsilon_{yy})/2$ component of the silicon strain for the four thicknesses from 5 to 40 nm. The black solid line marks the upper $d_p/2$ thick region. (b) Top view bidimensional map of the average strain in the upper $d_p/2$ thick region of the 5-nm-thick Si layer. The four quadrants report the four independent components of the strain tensor as calculated from the finite-element simulations. The lower edge is parallel to [100]. The island facets are superimposed for clarity. The side of the map is 110 nm wide. (c) Plot of $(\epsilon_{xx}+\epsilon_{yy})/2$ component of the strain in silicon as a function of depth along the island axis. The shaded zone is $d_p/2$ deep.

variations due to the specific geometry of the structure. In order to clarify these issues, we interpreted the results of the Raman spectra by comparison with three-dimensional strain maps generated by FEM.

The results of the modeling are reported in Fig. 3. Panel (a) displays the cross-sectional view of the $(\epsilon_{xx}+\epsilon_{yy})/2$ component of the strain for the (100) plane for all the four silicon layer thicknesses. The figure shows how the strain in the top $d_p/2$, marked by a black solid line, changes from highly tensile to nearly completely relaxed, moving from the thinnest to the thickest layer.[13,14] Panel (b) shows for the 5 nm sample the top view of an island, where the four quadrants map four independent components of the strain (after an adequate rotation $\epsilon_{yy}=\epsilon_{xx}$ and $\epsilon_{yz}=\epsilon_{xz}$) averaged within a depth of $d_p/2$, which in this case coincides with the thickness of the layer. As expected, the top of the island is almost biaxially stressed in the (001) plane, while the xz components become significant at the steepest facets. Panel (c) shows the in-plane strain over the (001) facets as a function of the depth in the Si layer. For the thicker layers, the strain is larger close to the Si/SiGe interface, whereas for the thinnest layers the geometry plays a more important role and the upper surface is the most strained.

A direct comparison of these results with the experimental spectra of Fig. 2 can be carried out by spectral simulation, summing up all the spectra generated by the individual finite elements.[15] In the most general case each individual spectrum consists of three Lorentzian curves centered at nondegenerate Raman shifts $\Delta\omega_1$, $\Delta\omega_2$, and $\Delta\omega_3$, which contribute to the total spectrum with their corresponding intensities I_1, I_2, and I_3, determined by the experimental geometry and the Raman tensors. In Fig. 2, the spectrum resulting from this simulation can be found superimposed to the actual experimental spectrum in order to test the validity of the model. For the case of the 5 nm layer, the comparison is strikingly coincident. The simulated spectra shown in this figure result only from the region on the top of the island, thus excluding the amount of layer directly over the substrate. This exclusion is the computational analog of the spectral subtraction (in this case without artifacts), and the inclusion of all the area would have resulted in an additional noninteresting band very close to that of relaxed silicon. The agreement for the centroid of the band is very high. Some uncertainties could have compensated each others because it was not possible to take into account parameters such as the spread in island dimension or to introduce in the spectral simulation the small shift induced by phonon confinement.[16] Nevertheless, beyond the centroid, also the shape of the band is very similar, and the trend as a function of the thickness is reproduced very accurately, as we will show in the next paragraphs.

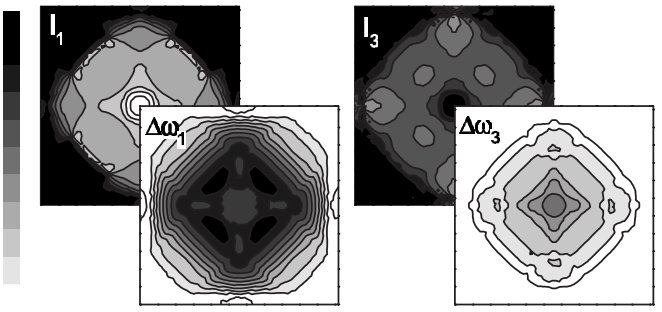

FIG. 4. Intensity I and relative Raman shift $\Delta\omega$ of the observable phonon as a function of the position of the dot. The colorbar is shown on the left. For the intensity I, black corresponds to 0 and white to 1. For the relative shift $\Delta\omega$, black corresponds to -15 cm^{-1} and white to 0 cm^{-1}. For clarity the components outside of the dot are set to 0 intensity.

FEM and spectral simulation are important also for the understanding of the physical origin of the band in the experimental spectrum. It is instructive to start the analysis from the simplified case of an island where the upper silicon cover is uniformly and biaxially stressed on each facet, with forces in the plane of the facet. In this case, the phonon degeneracy is removed, with one phonon perpendicular to the facet with an energy shift $\Delta\omega_1$, and two degenerate phonons in the plane of the facet $\Delta\omega_2$ and $\Delta\omega_3$. We can assign $\Delta\omega_2$ to the phonon in the (001) plane. Within this picture, in our experiment the selection rules state that $\Delta\omega_1$ is always observable, $\Delta\omega_2$ is always mute, and $\Delta\omega_3$ is observable only in the diagonal facets. This simplified case is quite similar to the situation described by the simulation.

Figure 4 reports $\Delta\omega_1$ and $\Delta\omega_3$, together with their corresponding intensities I_1 and I_3, as a function of the position on the dome. The inspection of $\Delta\omega_1$ shows that this phonon is responsible for the band observed in the experimental spec-

trum. All the phonon energies between 506 and 511 cm^{-1}, the spectral interval corresponding to the FWHM of the experimental band, are scattered from a region almost as wide as the diameter of the island. The measured in-plane strain is therefore well above 0.01 for a large area, making this sample attractive as a strained channel for high-mobility devices.[5] While I_1 is higher at those facets with a lower angle to the substrate, I_3 is more intense at the steeper facets. Although this phonon is in principle visible with our geometry (it is responsible for the lower shift band in the simulated spectrum), the shift $\Delta\omega_3$ is relatively small and is masked by the subtraction artifact. Nevertheless, the shoulder observed in the experimental spectrum can be attributed to this band. We can try to find a relationship between strain and shift by modifying the well-known formula for planar layers to $\Delta\omega_c = b_{\text{eff}}\langle\epsilon\rangle_{\text{in-plane}}$, where in this case $\Delta\omega_c$ is the centroid of the spectrum, $\langle\epsilon\rangle_{\text{in-plane}}$ is the average strain in the plane of each facet, and b_{eff} is the effective linear coefficient. For this experiment b_{eff} is 1300 cm^{-1}, a much higher value than the 750 cm^{-1} of planar films.[12] This result is an indication of the limits of validity of the planar approximation.

Going back to Fig. 2, we finally analyze similar samples with thicker silicon layers. The experimental spectra of the 10 and 20 nm are not as clean as the 5 nm, but they show a clear trend for the out-of-plane phonon that moves to lower strain with the increase in the cap layer thickness. The 40 nm sample is not reported because it shows a completely relaxed spectrum similar to the 0 nm. For the simulated spectra of the 10 and 20 nm samples, the agreement is less good than the 5 nm, but an explanation of this discrepancy could be the exceeding of the critical thickness and a partial plastic relaxation occurring in the silicon layer.[17] Nevertheless, the trend is very similar also in the simulated spectra: While the center of mass of the two-band spectrum moves to zero shift, the splitting of $\Delta\omega_1$ and $\Delta\omega_3$ reduces accordingly. In Fig. 2 we included also two curves, proportional to the functions $1/t$ and $1/t^3$, representing two models for the value of strain as a function of the layer thickness t. The results are closer to the $1/t$ function predicted by atomistic simulations in Ref. 18, with respect to the $1/t^3$ behavior resulting from analytical models of point stressors.[19]

IV. CONCLUSIONS

In conclusion, this paper provides an approach to characterize the strain in silicon layers on SiGe islands by a very sensitive experimental technique that now can also be better interpreted from a quantitative point of view. We showed that for a 5-nm-thick silicon layer the local strain produces a phonon energy shift detectable with resonant Raman spectroscopy. For thicker silicon layers, we observe a progressive reduction in the strain, which has been compared to previous theoretical and computational results. The direct comparison of FEM and experimental results with spectral simulation shows that the experimentally observed band originates from a large amount of the layer above the island. It is still possible to apply a linear relationship between strain and Raman shift similar to the one used for planar films, but the coefficient b_{eff} can be significantly different. In addition for this approximation it is better to modify the interpretation of the in-plane strain as the average component of the strain tensor in the plane of the facets. The specific case of a 5 nm Si cap layer is appealing for high-mobility applications because of the high in-plane strain exceeding 0.01.[20]

ACKNOWLEDGMENT

This work was supported by the EU (D-DOTFET, Project No. 012150).

[1] F. Capasso, Science **235**, 172 (1987).
[2] D. J. Paul, Semicond. Sci. Technol. **19**, R75 (2004); F. Schäffler, *ibid.* **12**, 1515 (1997).
[3] R. A. Donaton, D. Chidambarrao, J. Johnson, P. Chang, W. K. Liu, W. K. Henson, J. Holt, X. Li, J. Li, A. Domenicucci, A. Madan, K. Rim, and C. Wann, Tech. Dig. - Int. Electron Devices Meet. **2006**, 191; K. W. Ang, C. H. Tung, N. Balasubramanian, G. S. Samudra, and Y. C. Yeo, IEEE Electron Device Lett. **28**, 609 (2007); K. W. Ang, J. Lin, C. H. Tung, N. Balasubramanian, G. S. Samudra, and Y. C. Yeo, *ibid.* **55**, 850 (2008).
[4] L. Vescan, J. Cryst. Growth **194**, 173 (1998); O. G. Schmidt, N. Y. Jin-Phillipp, C. Lange, U. Denker, K. Eberl, R. Schreiner, H. Gräbeldinger, and H. Schweizer, Appl. Phys. Lett. **77**, 4139 (2000); J. J. Zhang, M. Stoffel, A. Rastelli, O. G. Schmidt, V. Jovanovic, L. K. Nanver, and G. Bauer, *ibid.* **91**, 173115 (2007).
[5] O. G. Schmidt and K. Eberl, IEEE Trans. Electron Devices **48**, 1175 (2001).
[6] A. Bernardi, M. I. Alonso, J. S. Reparaz, A. R. Goñi, P. D. Lacharmoise, J. O. Ossó, and M. Garriga, Nanotechnology **18**, 475401 (2007).
[7] M. Stoffel, U. Denker, G. S. Kar, H. Sigg, and O. G. Schmidt, Appl. Phys. Lett. **83**, 2910 (2003); M. Stoffel, G. S. Kar, U. Denker, A. Rastelli, H. Sigg, and O. G. Schmidt, Physica E (Amsterdam) **23**, 421 (2004).
[8] J. Stangl, T. Schülli, A. Hesse, V. Holy, G. Bauer, M. Stoffel, and O. G. Schmidt, Adv. Solid State Phys. **44**, 227 (2004).
[9] Z. Zhong, W. Schwinger, F. Schäffler, G. Bauer, G. Vastola, F. Montalenti, and L. Miglio, Phys. Rev. Lett. **98**, 176102 (2007).
[10] R. Gatti, F. Uhlik, and F. Montalenti, New J. Phys. **10**, 083039 (2008).
[11] J. B. Renucci, R. N. Tyte, and M. Cardona, Phys. Rev. B **11**, 3885 (1975).
[12] F. Pezzoli, E. Bonera, E. Grilli, M. Guzzi, S. Sanguinetti, D. Chrastina, G. Isella, H. von Känel, E. Wintersberger, J. Stangl, and G. Bauer, J. Appl. Phys. **103**, 093521 (2008).
[13] R. Marchetti, F. Montalenti, L. Miglio, G. Capellini, M. De Seta, and F. Evangelisti, Appl. Phys. Lett. **87**, 261919 (2005).
[14] G. Vastola, A. Marzegalli, F. Montalenti, and L. Miglio, Mat. Sci. Eng., B (to be published).
[15] E. Bonera, M. Fanciulli, and G. P. Carnevale, J. Appl. Phys. **100**,

033516 (2006).
[16] V. Paillard, P. Puech, M. A. Laguna, R. Carles, B. Kohn, and F. Huisken, J. Appl. Phys. **86**, 1921 (1999).
[17] J. H. Lin, Y. Q. Wu, J. Cui, Y. Fan, X. J. Yang, Z. M. Jiang, Y. Chen, and J. Zhou, J. Appl. Phys. **105**, 024307 (2009).
[18] M. A. Makeev and A. Madhukar, Phys. Rev. Lett. **86**, 5542 (2001).
[19] A. A. Maradudin and R. F. Wallis, Surf. Sci. **91**, 423 (1980).
[20] O. G. Schmidt, K. Eberl, and Y. Rau, Phys. Rev. B **62**, 16715 (2000).